CLAS-NOTE 2004-019

The Tagger Energy Scale: Interpreting the CMU Kinematic Fit Results

Daniel Sober , Hall Crannell and Franz J. Klein
The Catholic University of America
18 June 2004

Abstract

This note explains the structure of the tagger photon energy correction obtained for the 3.115 GeV portion of the g1c run period by the kinematic fit of CLAS-Note 2004-017, and suggests how this energy correction can be generalized to other run periods.

1 Introduction

In CLAS-Note 2004-017 [1], Mike Williams *et al.* (Carnegie Mellon University) present the results of the CLAS Kinematic Fit applied to the reaction $\gamma p \to \pi^+\pi^- p$ for the 3.115 GeV portion of the g1c run period. Among their results is a correction to the tagged photon beam energy (Figure 9 of [1]) showing a "double-humped structure [which] is not understood." The purpose of this note is to explain how the shape of this photon energy correction is related to physical alignment parameters of the tagger focal plane, and to suggest how these kinematic fit results can be used as a basis for tagger energy corrections for other run periods.

2 The kinematic fit results

Figure 1 shows the photon energy corrections of Ref. [1] plotted as $\Delta(k/E_0)$ versus nominal k/E_0. (Figure 9 of [1] shows the same data in the form $\Delta(E_\gamma)$ versus E_γ;

this note will use the symbol k instead of E_γ to represent the photon energy.) The data points were fitted to bins approximately 26 MeV (0.0083 E_0) wide. Note that the energy channel width of the tagger is approximately 0.001 E_0, which is comparable to the structure revealed by the kinematic fit. The dashed lines in Figure 1 indicate the channel width. The solid curve is the fit by the CMU group using a piecewise quadratic function

$$\Delta(k/E_0) = A + B(k/E_0) + C(k/E_0)^2 \tag{1}$$

with coefficients given by Table 1.

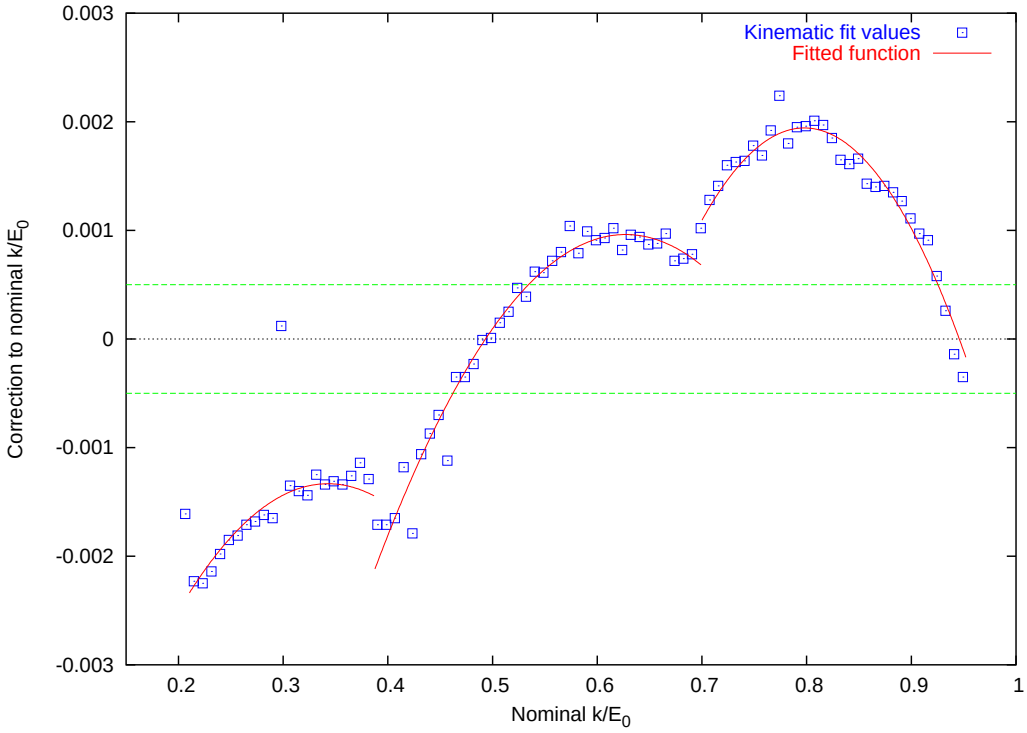

Figure 1: Tagger energy correction calculated using kinematic fit in Ref. [1], converted to units of k/E_0. The curve is the piecewise polynomial fit of Ref. [1]. The horizontal lines indicate the average tagger channel width of 0.001 E_0.

The energy boundaries between the regions were estimated by the authors of [1] to be at k/E_0= 0.401 and 0.674. The values 0.387 and 0.700 in Table 1 are based on the structure of the focal plane as described in the following section.

Table 1: Empirical fit to photon energy correction of Ref. [1], converted from Δk vs. k to $\Delta(k/E_0)$ vs. k/E_0.

Energy region	A	B	C
$k/E_0 < 0.387$	-0.0080760	0.0393665	-0.0574313
$0.387 < k/E_0 < 0.700$	-0.0201725	0.0674121	-0.0537556
$k/E_0 0.700$	-0.0545486	0.141611	-0.0887460

3 The structure of the tagger focal plane

The tagger focal plane is instrumented with 384 "E-counters", which determine the precise energy of the tagged photon, and 61 double-ended "T-counters" which provide fast timing information. Each E-counter subtends an energy bite of approximately $\Delta(k/E_0) \simeq 0.003$, and the counters overlap by approximately 1/3 in the plane normal to the electron trajectories, so that using alternating coincidences and anticoincidences between neighboring E-counters provides 767 fine channels with an energy resolution of $\Delta(k/E_0) \simeq 0.001$, covering the range $0.20 < k/E_0 < 0.95$. The E-counters are numbered in order of increasing electron momentum (and thus of decreasing photon energy), with E_1 corresponding to $k/E_0 \simeq 0.95$ and E_{384} to $k/E_0 \simeq= 0.20$.

The individual E-counters are plastic scintillation counters of thickness 4 mm, length 200 mm, and transverse widths which vary from 18 mm to 6.0 mm in order to subtend a constant energy bite. Since the electron trajectories cross the focal plane at small angles (varying from 25.9° to 9.4°), the E-counters are aligned in an open Venetian-blind-like geometry (Figure 2), and are spaced at intervals of approximately 1 inch (25 mm) along a focal plane of total length 30.5 feet (9.3 m). One end of each E-counter is glued to a flexible optical-fiber light guide. The photomultiplier tubes are supported independently of the E-counters.

The aluminum frame containing the focal plane instrumentation was manufactured in four sections of length $\simeq$ 12.5 feet (3.81 m) each. These sections were then bolted to each other and to the flange of the extended vacuum box which was previously welded to the tagger magnet. The ends of the E-counter scintillators fit into slots machined into pairs of aluminum "rails" which are made from aluminum angle of dimension 3 inches by 3 inches by 3/16 inch thick. The first two rails, which contain counters E_1 – E_{133} ($0.70 \leq k/E_0 \leq 0.95$) and E_{134} – E_{293} ($0.39 \leq k/E_0 \leq 0.70$) respectively, are of length 149.8 inches, and are attached to the frame by bolts located 1.5 inches from

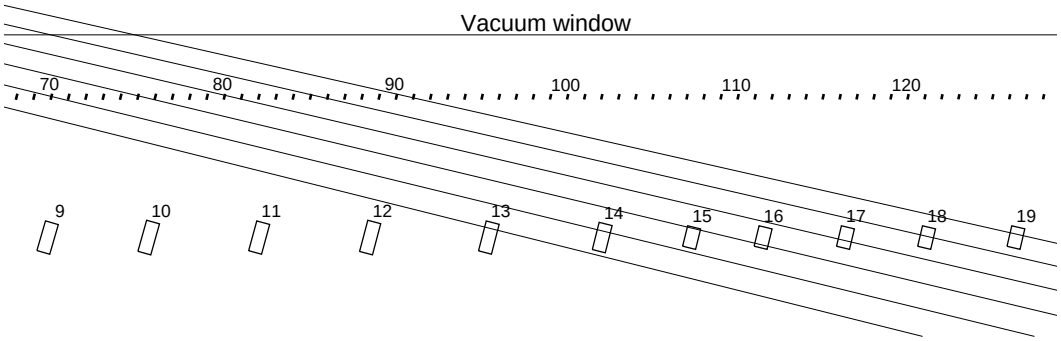

Figure 2: Relative positions of E-counters, T-counters, and electron trajectories (Figure 5 of Ref. [2].) This section of the focal plane contains E-counters 68-128 and T-counters 9-19.

each end. The third rail, containing E_{294} – E_{384} ($0.20 \leq k/E_0 \leq 0.39$), is only 85 inches long, and is supported by bolts at 1.5 inches and 74.8 inches from the upstream end.

The "cusps" observed in the energy correction function of Figure 1 occur at photon energies corresponding to E-counters E_{133} and E_{293}, *i.e.* at the transitions between adjacent support rails. It is thus easy to interpret the structure of Figure 1 as resulting from the gravitational deflection of the E-counter rails between their support points. A simple calculation of this deformation, neglecting the weight of the scintillators, gives a maximum deflection of about 1.8 mm at the center of rails 1 and 2, and about 0.11 mm for rail 3 , whose support points are only half as far apart (the maximum deflection scales as *(length)*^{4}). The weight of the scintillators is only about 10% of the weight of the rails, and some of the scintillator weight is supported by the light guides. We have also neglected the fact that the rails are inclined at approximately 22° to the horizontal.

(a)

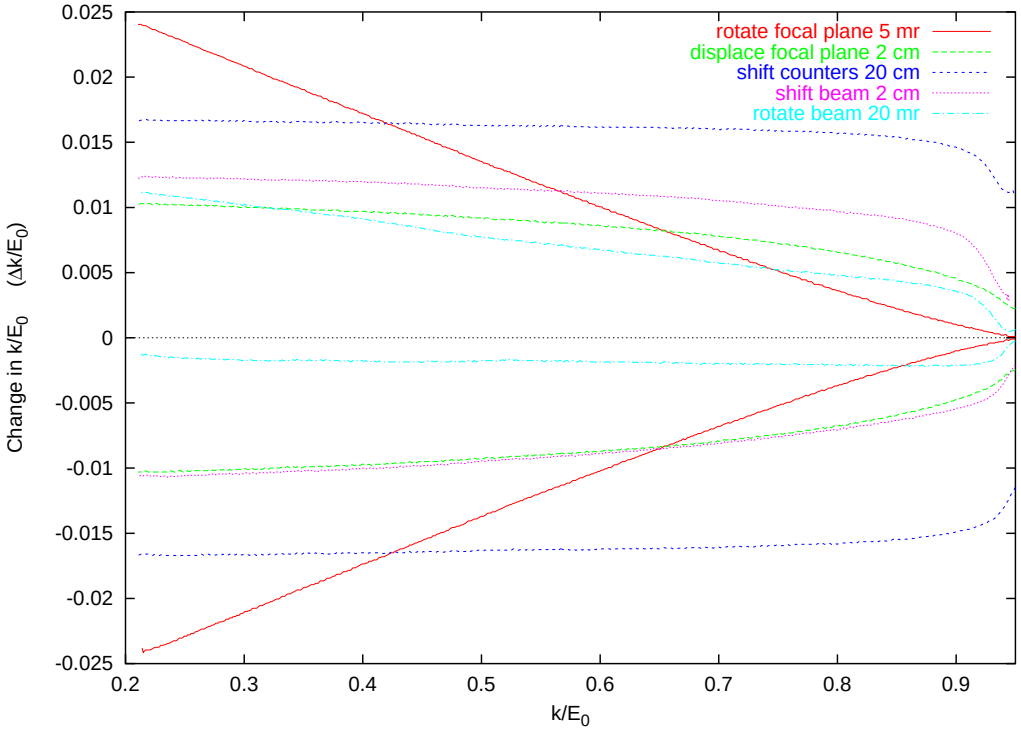

(b)

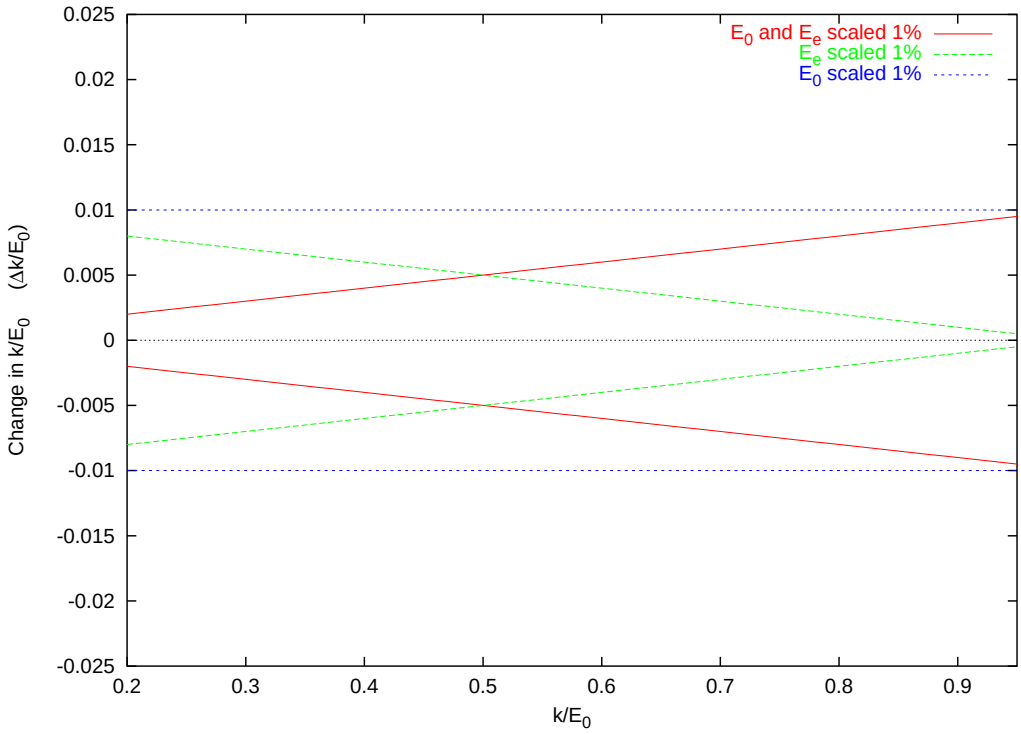

Figure 3: Calculated tagger energy shifts (a) due to hypothetical spatial shifts and rotations, (b) due to hypothetical shifts in beam energy and tagger momentum scales.

4 Tagger calculations

We have performed simulations of the effects of gravitational sag and various possible misalignments of the tagger focal plane using a Monte Carlo code `tagc_ray` in which electron trajectories are generated at the radiator with the appropriate energy and angular distributions, and are then propagated through the tagger magnet field to the tagger focal plane, where the hit pattern of E and T counters is determined. The propagation through the magnetic field is performed by means of ray-tracing code extracted from the program `SNAKE` [3], using the field maps of the tagger magnet performed at 10 excitation currents (corresponding to beam energies $E_0 = 0.449$, 0.899, 1.795, 2.388, 2.980, 4.144, 5.188, 5.563, 5.867 and 6.120 GeV) by the CUA group in 1993.

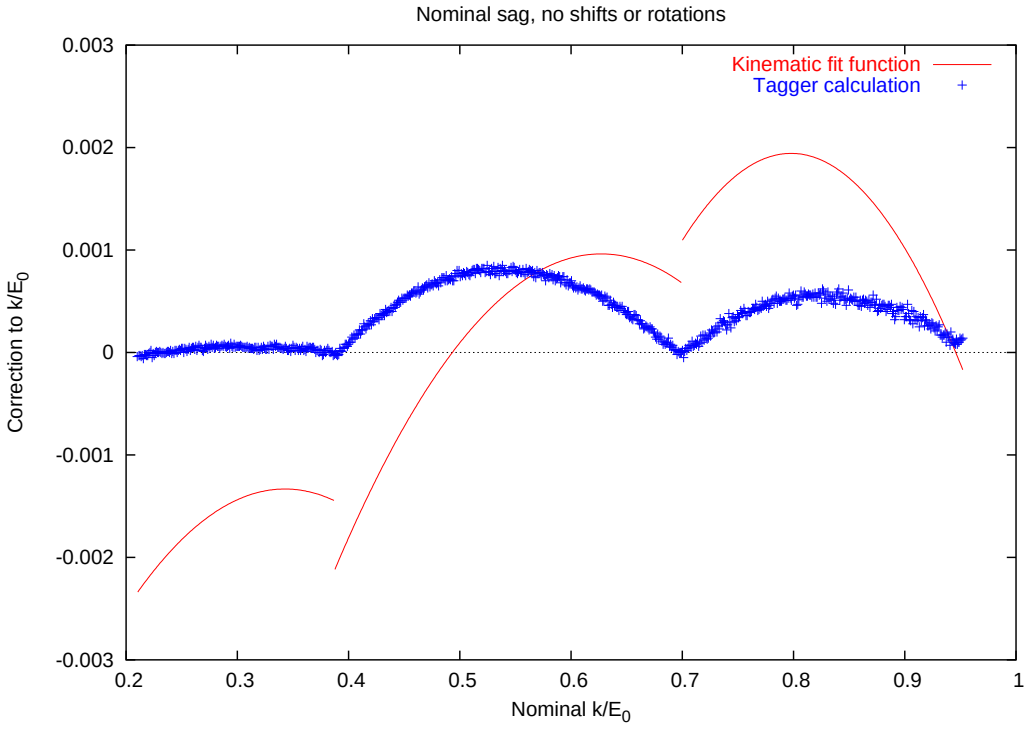

Figure 4: Calculated tagger energy shifts due to nominal gravitational sag of the 3 pairs of E-counter rails. The curve is the fit of Ref. [1].

The nominal tagger energy scale is based on previous calculations using a version of this code. The boundaries and average value of k/E_0 for each of the 767 fine channels, tabulated for all 10 excitation currents, are in the file `tagE-boundaries_ALL.dat`. The standard tagger package searches this file and uses the data set corresponding to the

E_0 value closest to that of the run being analyzed. Since the k/E_0 boundaries of a given channel vary only slowly with E_0, no more elaborate interpolation process is necessary. For example, compared to $E_0 = 2.980$ GeV, the maximum change in k/E_0 for a given channel is 0.0019 at 1.795 GeV, 0.0009 at 4.144 GeV, 0.0047 at 5.189 GeV, and 0.0127 at 6.120 GeV. The largest deviations occur at the low-k end of the focal plane: in the high-counting-rate region, corresponding to counters T_1–T_{19} ($0.77 \leq k/E_0 \leq 0.95$), the maximum deviations are 0.0002, 0.0000, 0.0006 and 0.0030 respectively. If precision at the level of 10^{-3} is required for $E_0 > 4$ GeV, an interpolation in E_0 could be implemented instead of using the closest value of E_0. (A new version of `tagE-boundaries_ALL.dat` with spline-interpolated data for 68 values of E_0 is available for testing.)

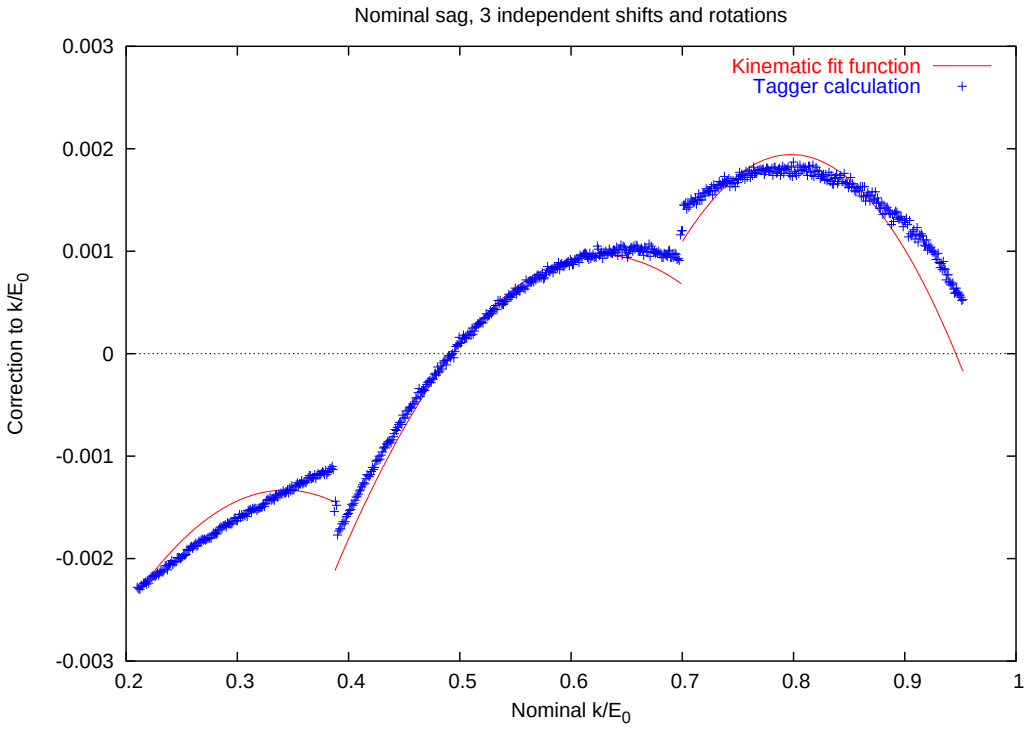

Figure 5: Calculated tagger energy shifts due to nominal gravitational sag plus empirical shift and rotation of each pair of E-counter rails. The curve is the fit of Ref. [1].

For the present calculations, the deformation and misalignment of the the E-counter rails was implemented by generating new files of E-counter position to replace the standard input file `E-CTRS.DAT`. Other perturbations, such as global shifts and rotations of the whole focal plane or shifts in beam energy, can be generated by changing parameters within the `tagc_ray` code. Figure 3, calculated before the kinematic fit results

were available, shows the effects of various hypothetical global misalignments and energy shifts on the tagger energy scale; it does not include the possibility of deformation of the E-counter rails.

Figure 4 shows the effect of the nominal gravitational sag of the 3 E-counter rails (1.8 mm, 1.8 mm and 0.11 mm respectively, parameterized by a parabolic shape), compared to the energy correction of Ref. [1]. It is seen that, while the "cusps" are in the correct positions, the fit is qualitatively poor, although, as shown in Table 2, the standard deviation from the function of Ref. [1] is only 0.00119, or about one tagger channel. A considerable improvement (Figure 5) can be made by allowing each of the E-counter rails to have an independent rotation and shift relative to its nominal position; this was parameterized by changing the y-coordinate of the bolt hole at each end of the rail relative to its nominal position. Table 2 shows the bolt positions for each rail, as well as the assumed sags and the standard deviation of the calculated 767 fine-channel energies from the kinematic fit function. While the calculated energy shifts for Rail 2 are in good agreement with the kinematic fit data, the other two rails exhibit more curvature than is predicted by the nominal sag.

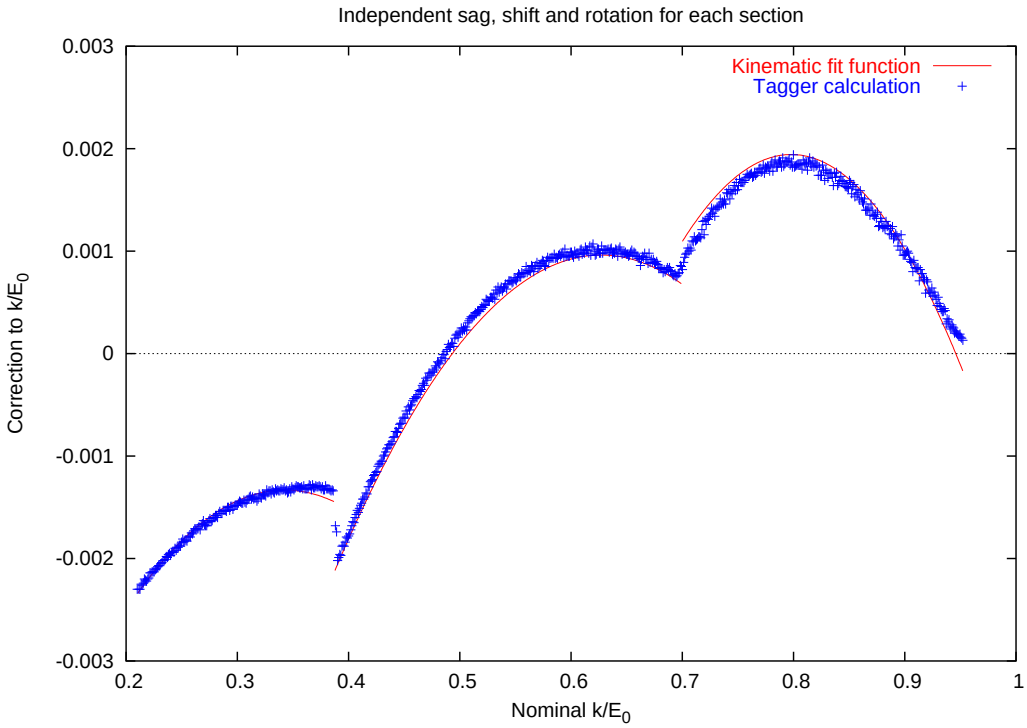

Figure 6: Calculated tagger energy shifts due to empirical sag, shift and rotation of each pair of E-counter rails. The curve is the fit of Ref. [1].

Since the straightness of the rails was specified only to be better than 0.1 inch before machining, it is possible that the actual sag of the rails exceeds the value calculated for gravitational deformation alone. Thus it is not unreasonable to consider varying the deformation of each rail as a free parameter together with rotation and shift. Doing this (Figure 6) gives a result which is in excellent agreement with the kinematic fit data.

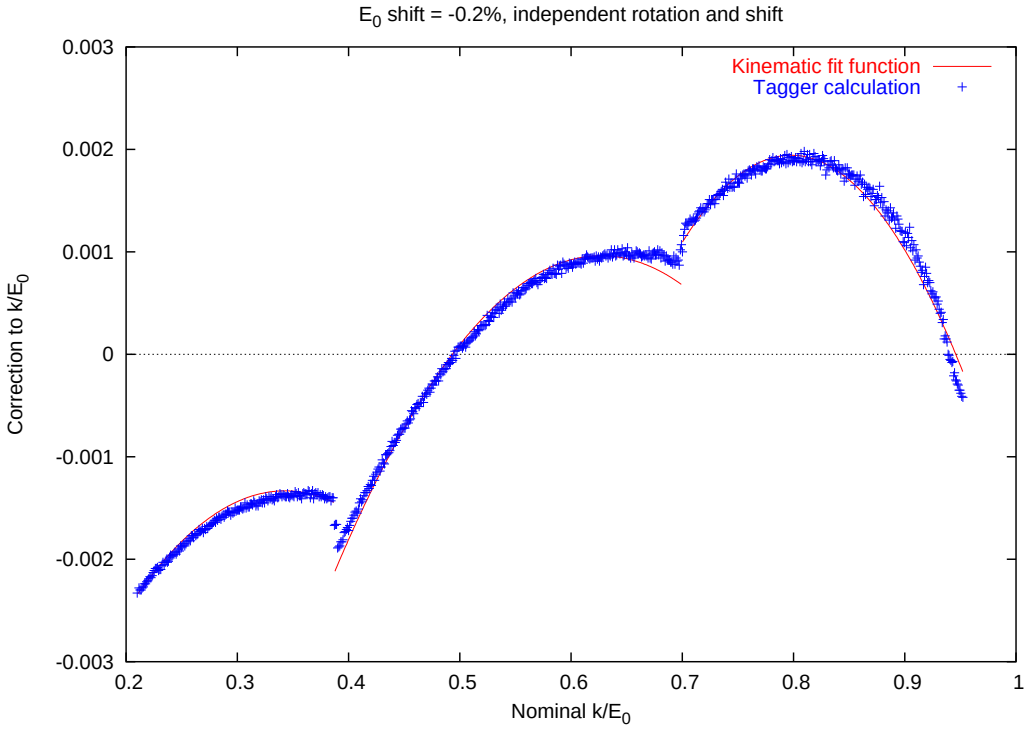

Figure 7: Calculated tagger energy shifts including an assumed shift of -0.2% in incident beam energy, plus empirical sag, shift and rotation of each pair of E-counter rails. The curve is the fit of Ref. [1].

A possible concern about the kinematic fit procedure of Ref. [1] is that the incident electron beam energy E_0 was taken as the nominal value of 3.115 GeV provided by MCC to the EPICS data stream. When precise energy measurements are performed in Hall A, they usually yield values of E_0 which are 0.1% to 0.3% lower than the nominal energy from MCC. Unfortunately, no Hall A energy calibration appears to have been done during the 3.1 GeV `g1c` run time. The table of pull quantities in [1] appears to show that the kinematic fit resulted in an overall adjustment of E_γ by about 2 MeV. It is not clear to us how the results of this fit might have been changed if a precise beam energy measurement had been available. In the absence of a precise measurement of

E_0, we have simulated the effect of a shift of -0.2% in E_0, assuming that the tagger magnet field tracks the incident beam energy correctly. We have varied the positions and angles of all 3 E-counter rails, and also given an empirical sag to Rail 3. The results are shown in Figure 7. The fit is excellent, but with the disturbing feature that the required displacements of the E-rail bolts range up to 13 mm, which we feel is far outside the alignment uncertainty.

Table 2: Parameters of several tagger calculations which are compared with the kinematic fit function in Figures 4–7. The Δy values indicate the assumed distance below the nominal value for each bolt supporting the ends of the E-counter rails. σ is the standard deviation of the tagger calculation from the kinematic fit function, averaged over the 767 fine channels.

		Rail 1 ($k/E_0 > 0.70$)			Rail 2 (0.39 - 0.70)			Rail 3 ($> k/E_0 < 0.39$)			
Fig.	ΔE_0 (%)	max. Sag (mm)	Δy Bolt 1 (mm)	Δy Bolt 2 (mm)	max. Sag (mm)	Δy Bolt 1 (mm)	Δy Bolt 2 (mm)	max. Sag (mm)	Δy Bolt 1 (mm)	Δy Bolt 2 (mm)	σ (% of E_0)
4	0	1.8	0	0	1.8	0	0	0.11	0	0	0.119
5	0	1.8	4.03	3.66	1.8	2.42	-3.53	0.11	-2.30	-4.16	0.019
6	0	5.0	-1.33	2.40	2.5	1.92	-4.03	0.50	-2.71	-4.01	0.009
7	-0.2	1.8	13.60	6.72	1.8	5.81	-2.20	0.50	-1.30	-3.16	0.009

5 Conclusions

Ignoring the question of the correct value of incident beam energy, it would be reasonable to take the parameters corresponding to Figure 6 as an excellent description of the physical layout of the tagger focal plane, and then re-compute the tagger energy scale for all 10 field maps.

Unfortunately, the kinematic fit of Ref. [1] was done for a data set for which no Hall A energy calibration exists. We do not know to what extent the calculated shift in E_γ in [1] can be used as a substitute for a reliable measurement of E_0. Until a full kinematic fit like that of [1] is done for a data set with a well-calibrated incident beam energy (and, ideally, with the newly installed Hall probe in the tagger magnet), we do not have a definitive solution to this problem. The recently measured relative energy calibration data taken with the Primex pair spectrometer may add some important constraints when their analysis is complete.

References

[1] M. Williams, D. Applegate and C.A. Meyer, "Determining Momentum and Energy Corrections for g1c using Kinematic Fitting," CLAS-Note 2004-017 (2004).

[2] D.I. Sober *et al.*, "The bremsstrahlung tagged photon beam in Hall B at JLab," Nucl. Instr. and Meth. A **440**, 263 (2000).

[3] Program `SNAKE`, Pascal Vernin, private communication. (Original code obtained from John LeRose.)